MOLECULAR AND CELLULAR BIOLOGY, Oct. 1996, p. 5896–5904 Vol. 16, No. 10
0270-7306/96/$04.00+0

Length Changes in the Joining Segment between Domains 5 and 6 of a Group II Intron Inhibit Self-Splicing and Alter 3′ Splice Site Selection

SCOTT C. BOULANGER,[1] PEGGY HO FAIX,[2] HAIYAN YANG,[2] JIN ZHUO,[2] JAMES S. FRANZEN,[2] CRAIG L. PEEBLES,[2] AND PHILIP S. PERLMAN[1]*

Department of Biochemistry, University of Texas Southwestern Medical Center, Dallas, Texas 75235-9148,[1] and Department of Biological Sciences, University of Pittsburgh, Pittsburgh, Pennsylvania 15260-7700[2]

Received 31 January 1996/Returned for modification 1 April 1996/Accepted 22 July 1996

Domain 5 (D5) and domain 6 (D6) are adjacent folded hairpin substructures of self-splicing group II introns that appear to interact within the active ribozyme. Here we describe the effects of changing the length of the 3-nucleotide segment joining D5 to D6 [called J(56)3] on the splicing reactions of intron 5γ of the *COXI* gene of yeast mitochondrial DNA. Shortened variants J(56)0 and J(56)1 were defective in vitro for branching, and the second splicing step was performed inefficiently and inaccurately. The lengthened variant J(56)5 had a milder defect—splicing occurred at a reduced rate but with correct branching and a mostly accurate 3′ splice junction choice. Yeast mitochondria were transformed with the J(56)5 allele, and the resulting yeast strain was respiration deficient because of ineffective aI5γ splicing. Respiration-competent revertants were recovered, and in one type a single joiner nucleotide was deleted while in the other type a nucleotide of D6 was deleted. Although these revertants still showed partial splicing blocks in vivo and in vitro, including a substantial defect in the second step of splicing, both spliced accurately in vivo. These results establish that a 3-nucleotide J(56) is optimal for this intron, especially for the accuracy of 3′ splice junction selection, and indicate that D5 and D6 are probably not coaxially stacked.

Self-splicing group II introns are comprised of six secondary structure domains tethered by joining segments with an undefined secondary structure (23, 24). Domain 5 (D5) is a highly conserved 34-nucleotide (nt) hairpin located near the 3′ end of group II introns. It is well-established that D5 of intron aI5γ from *Saccharomyces cerevisiae* mitochondrial DNA (mtDNA) plays a crucial role in self-splicing (23). Both *cis* and *trans* splicing assays have shown that D5 is required for the first splicing step, release of exon 1 (E1). Several recent studies have shown that D5 is also required for the second splicing step, in both forward (7) and reverse (34) directions. *trans* splicing experiments first showed that D5 has a binding site in the upstream region of the intron (18); D5 binding is mediated by tertiary interactions involving some specific ribose 2′-OH and phosphate groups of the D5 RNA backbone (1, 7). By deleting other intron domains, it was found that domain 1 (D1) contains important elements of the D5 binding site (21), and recently, a region of D1 that appears to interact with the tetraloop of D5 has been identified (9). Biochemical studies have shown that D5 binds to substrate RNAs with a K_m of about 330 nM and catalyzes the release of E1 with multiple turnovers (12, 31, 36).

Domain 6 (D6) contains the branchpoint adenosine (*A*-880 in intron aI5γ) that attacks the 5′ splice junction (5′SJ) in the first step of the splicing reaction (38). Although D6 is far less conserved in both primary sequence and secondary structure than D5, the branchpoint is typically present as a bulged residue between the fourth and fifth base pairs from the base of D6 and either 7 or 8 nt from the 3′ splice junction (3′SJ) (6, 17, 23, 24). This conserved position for D6 and the branchpoint hints that they may play a role in defining the 3′SJ. Several tertiary interactions that influence reaction at the 3′SJ in vitro (δ-δ′ and γ-γ′) have been identified previously (6, 17). Recently, we have found that an Rp phosphorothioate at the 3′SJ of aI5γ blocks its use in splicing (27). Significantly, that atomic replacement did not lead to splicing at alternative sites, showing that no other location is readily activated for step 2 of splicing by a properly folded transcript. However, mutant transcripts lacking D6 perform the second splicing reaction with reduced fidelity (15, 21), suggesting that those mutations alter the configuration of the active site in the second step.

With *trans* assays to determine D5 function, it was found that D5 positions D6 for its role in the first step of the reaction and that attachment to D5 influences branching and 3′SJ preference when D6 and the second exon are present (10). Thus, D5 of group II introns is a critical catalytic segment that specifically interacts with D6 to position the branchpoint adenosine for the first step of splicing. D5 has been compared with helix I, a secondary structure formed in the spliceosome between U2 and U6 small nuclear RNAs (22), while D6 resembles the branchpoint helix formed between U2 small nuclear RNA and the pre-mRNA (14). Those two spliceosomal helices are connected by an unstructured joiner in the U2 small nuclear RNA sequence that might then correspond to the joiner connecting D5 to D6 in group II introns.

The number of nucleotides in the joining segment between D5 and D6 [hereafter termed J(56)] exhibits some variation among group II introns (24). In group IIA introns, the most frequent length for J(56) is 2 nt, with the dinucleotide GG being the most common sequence. In group IIB introns (the subgroup including aI5γ), the length of J(56) varies from 2 to 5 nt, with 3 nt being the most frequent. Unlike group IIA introns, the sequence of J(56) in group IIB introns is not highly conserved, although the residue adjacent to D5 is often a U. There are no predicted tertiary interactions between J(56) and any other region of the intron.

Because the D5 and D6 helices are separated by just 3 nt in

* Corresponding author. Phone: (214) 648-1464. Fax: (214) 648-1474. Electronic mail address: perlman@utsw.swmed.edu.

TABLE 1. Rates of self-splicing by joiner variant transcripts

RNA (joiner sequence)	Result for[a]:					
	1.5 M KCl			1.5 M $(NH_4)_2SO_4$		
	k (min^{-1})	f_{active}	r^2	k (min^{-1})	f_{active}	r^2
J(56)0	0.37	0.34	0.99	0.011	0.50[b]	>0.99
J(56)1 (A)	0.29	0.28	0.82	0.012	0.47	0.99
J(56)2 (UA)	0.17	0.39	0.99	0.015	0.55	>0.99
J(56)3 (UUA) (wild type)[c]	0.18	0.53	>0.99	0.30	0.59	0.96
	0.20	0.43	>0.99	0.29	0.53	0.94
J(56)5ΔU (UAUA)	0.23	0.32	0.99	0.17	0.48	0.94
J(56)5ΔC (UUAUA)	0.25	0.36	0.83	0.15	0.52	0.97
J(56)5 (UUAUA)	0.21	0.38	0.95	0.025	0.52	0.99

[a] The rate coefficients (k) and fractions of active transcripts (f_{active}) are shown for timed experiments at 45°C in splicing buffer containing either KCl or $(NH_4)_2SO_4$. The equation used for fitting to the total amount of products accumulated at various times t was $[(\Sigma products)_t/(\text{full-length transcript})_{t=0}] = f_{active}(1 - e^{-kt})$. The KCl trials were fitted for observations for 0 through 32 min, while the $(NH_4)_2SO_4$ experiments were fitted to data for 0 through 64 min. r^2 is the regression coefficient of curve fitting as calculated with the DeltaGraph software.

[b] The fraction active (f_{active}) could not be determined independently in this experiment because of the low rate of splicing, so a reasonable value of 0.50 was used as a fixed parameter value for curve fitting.

[c] Two wild-type transcript preparations were analyzed independently.

aI5γ, we speculated that these two domains might interact via helix stacking (10). A stacked interaction between adjacent helices was first demonstrated in tRNAs (20) and is now known for other RNAs, including the hammerhead ribozyme (33) and self-splicing group I introns (26). In the absence of any evidence favoring stacking between D5 and D6, it also seemed plausible that these two largely helical domains might interact in some parallel or side-by-side fashion (10).

Here we analyze the splicing phenotypes of variants of aI5γ in which the length of J(56) is either increased or decreased. Our observations indicate that the length of the tether connecting D5 to D6 is important for the rate of self-splicing, for branching efficiency in the first step of splicing, and for accurate 3′SJ definition. By using mitochondrial transformation it was found that the joiner length is also an important parameter in vivo. These results establish that the 3-nt J(56) is optimal for the splicing of this intron.

MATERIALS AND METHODS

Plasmids and transcription templates. Plasmid pJD20 was the template for transcription of the wild-type precursor RNA (18). Plasmids pJD20-J(56)0, pJD20-J(56)1, pJD20-J(56)2, and pJD20-J(56)5 are variants of pJD20 with the designated J(56) mutations. Plasmids pJD20-J(56)5ΔU and pJD20-J(56)5ΔC are derivatives of pJD20 constructed with the revertant sequences recovered from the J(56)5 transformant. Wild-type D56 RNA was transcribed from a template prepared by PCR with the pair of primers CP92-112 (5′-TAATACGACTCAC TATAGGGAGCCGTATGCGATGAAAG-3′) and CP92-113 (5′-ATCCCGAT AGGTAGACCTTTACAAG-3′) plus an input of plasmid DNA. The resulting D56 template includes the preferred T7 RNA polymerase promoter, initiating with a 5′-GG dinucleotide followed by D5, J(56)3, and D6 and ending with the sequence 5′-GAU at the natural 3′ end of the intron. Other D56 RNAs were made in the same way from the mutant allele plasmids. Transcripts containing just D5 or D6 were transcribed from synthetic, partly double-stranded templates (12, 25). Plasmid pJD-I3′-673 was the template for transcription of the E1:D123 RNA (18) that was used in the *trans* splicing experiments.

Self-splicing experiments. Transcripts were made with T7 RNA polymerase and recovered from Sephadex-G50 spun columns for in vitro splicing reactions. D5, D6, D56, and E1:D123 RNAs were fractionated on 20% polyacrylamide gels and eluted from gel slices. Purified transcripts were stored frozen in water. For self-splicing experiments, transcripts were incubated in splicing reaction buffer containing either 20 mM HEPES (*N*-2-hydroxyethylpiperazine-*N*′-2-ethanesulfonic acid [pH 7.5]), 100 mM $MgSO_4$, or 100 mM $MgCl_2$ and either 1.5 M $(NH_4)_2SO_4$ or 1.5 M KCl (19, 21). For *trans* reactions, 30 nM E1:D123 and 600 nM D56 were incubated in 1.0 M KCl or 1.0 M NH_4Cl reaction buffer (31). Reaction mixtures were incubated at 45°C, the reactions were stopped by the addition of 10 μl of 0.1 M EDTA, and the mixtures were fractionated through 4% polyacrylamide gels. The results were determined by autoradiography and quantitated by scanning with either a Molecular Dynamics PhosphorImager or an Ambis model 4000 Radioanalytic Imaging System. Apparent first-order rate constants and the fraction of active transcripts were calculated after fitting time-series data for six (or more) timed reactions (ranging from 1 to 64 min) to a two-component model for full-length transcripts (see Table 1 footnotes). This model assumes that some molecules are folded correctly and therefore are able to react without delay, while the remaining transcripts are not reactive. For the transcripts analyzed here, the fraction of active RNA ranged from 45 to 60% for experiments with the 1.5 M $(NH_4)_2SO_4$ reaction buffer and from 28 to 53% for experiments with the 1.5 M KCl reaction buffer (Table 1). The fitting calculations were done with the DeltaGraph version 3.5 (DeltaPoint) software package.

Thermal denaturation. Thermal denaturation of D5, D6, and D56 RNAs was monitored at 260 and 280 nm with ramp rates of 1°C min^{-1} with an AVIV-14DS spectrophotometer equipped with a Peltier cooling-heating cuvette jacket (13, 31). The maxima of the temperature-derivative curves of the hyperchromicity profiles were defined as the characteristic transition temperatures for each RNA sample. The experimental variation of these transition temperatures was within ±1°C. The samples had nominal A_{260} values of 0.5 at 0°C. All meltings were done in 1.0 M KCl–20 mM HEPES (pH 7.0)–0.5 mM EDTA.

Mitochondrial transformation and genetic procedures. Mitochondrial transformation was done with materials and by the overall procedures previously described (4, 5, 28). A [*rho*^{0}] derivative of strain DBY947 (*MAT*α *ura3-52 ade2-101*) was shot with 0.5-μm gold beads coated with a mixture of plasmids pJD20-J(56)5 and YEp352 (a *URA3* episomal plasmid). Ura$^+$ transformants were selected and screened for mitochondrial transformants by a test cross to strain C2159, a *mit*$^-$ mutant with a point mutation in D1 of aI5γ (2). Sectors of Ura$^+$ cells that could restore C2159 to growth on glycerol were subcloned and screened again by the test cross until the pMIT (a synthetic petite mutant) mitochondrial transformant was purified. The splicing phenotype of the J(56)5 allele of aI5γ was initially determined by a test cross to a *mit*$^-$ mutant, C1067, which has two point mutations in D5 and two more in D6; that cross yielded no Gly$^+$ progeny, indicating that the J(56)5 mutation blocks splicing.

The J(56)5 mutant allele of aI5γ was transferred to an intact mitochondrial genome by mating the pMIT to the [*rho*$^+$] strain MY375 (*MAT***a** *ura3-52 his4*Δ*34 kar1*) with the mtDNA of strain GII-5γ, in which the *COXI* gene has three introns (aI3α, aI4α, and aI5γ). Mated cells were plated on solid medium containing uracil and adenine to exclude haploid progeny with the nuclear genome of strain MY375, and the resulting colonies were screened to identify the desired haploid Gly$^-$ (*mit*$^-$) recombinants with the nuclear genome of strain DBY947. The resulting strain, 947/GII-5γ-J5, was confirmed to contain the J(56)5 mutation by DNA sequencing after PCR amplification of the intron from mtDNA. Revertants were isolated from red papillae (due to the *ade2* marker) growing on the surface of tan colonies on YEPD plates (32).

RNA filter hybridization. Yeast strains were grown in 50-ml cultures of YEP medium containing 2% raffinose to an A_{600} of 2 to 5. Cultures were harvested, and cellular RNA was prepared as described previously (37) except that the suspension of lysed yeast cells was frozen in liquid nitrogen rather than dry ice-ethanol. Samples containing 50 to 75 μg of RNA were analyzed on 1.2% agarose gels containing 6% formaldehyde. Northern (RNA) blots were done as described previously (4). Probes were prepared by using a random-primed labeling kit (BMB, Inc.) with cloned restriction fragments of mtDNA as templates. The following fragments were used: the 2.7-kb *Pst*I *COXII* fragment from pMT36 (35), the 1.1-kb *Acc*I-to-*Cla*I aI1 fragment from pSH2, the 0.9-kb *Taq*I-to-*Bam*HI aI5γ fragment from pSDH5γIVS (21), and the 0.46-kb *Bcl*I-to-*Eco*RI *COXI* fragment from pBS(−)SER (28) that detects both exons flanking aI5γ.

Amplification and primer extension methods. The sequences of the 3′ ends of aI5γ in site-directed mutants, transformants, and revertants were determined after PCR amplification with primers CP92-112 and CP90-305 (see above) with

plasmid or cellular DNA templates followed by dideoxynucleotide chain-terminated sequencing (Sequenase; Amersham) from primer CP90-305. Spliced exons in wild-type or mutant mitochondrial RNA extracted from the J(56)5 strain or its revertants were converted to cDNAs by reverse transcription (RT)-PCR with primers CK90-202 (5′-CACAATGGGTGGTTTAACTGG-3′) and CP90-305, cloned in plasmid pUC119, and sequenced. Spliced exon sequences were determined by a similar strategy from self-splicing reactions in 1.5 M KCl reaction buffer of wild-type or mutant pre-mRNAs. Gel-purified PCR products were also sequenced, without cloning, with end-labeled primers (CircumVent Thermal Cycle Sequencing; New England Biolabs).

For the RT-primer extension experiment for which the results are shown in Fig. 3, an unlabeled sample of the transcript for each J(56) allele was incubated in reaction buffer containing 1.5 M KCl for 40 min at 45°C. Then, the 5′-end-labeled 3′-exon-specific primer, yeast tRNA carrier, sodium acetate, and diethyl pyrocarbonate (DEPC)-treated water were added, and the nucleic acids were precipitated with ethanol. The pellet was dissolved in 30 μl of hybridization buffer (1 M NaCl, 0.15 M HEPES [pH 7.5], 1 mM EDTA) and incubated for 4 h at 30°C. After ethanol precipitation, each sample was dissolved in 25 μl of freshly prepared RT mix (5 μl of 5× avian myeloblastosis virus RT reaction buffer [Promega], 1.5 μl of deoxynucleoside triphosphate mix that contained 10 mM (each) deoxynucleoside triphosphate, and 18.5 μl of DEPC-treated water). To each reaction mixture, 2 μl of avian myeloblastosis virus reverse transcriptase (25 U/μl; Promega) was added before incubation at 55°C for 15 min. Reactions were stopped by the addition of 1 μl of 0.5 M EDTA before treatment with RNase A (2 mg/ml) at 37°C for 30 min. Nucleic acids were precipitated with ethanol and dissolved in 6 μl of Tris-EDTA plus 6 μl of Sequenase stop buffer, and aliquots were analyzed on sequencing gels adjacent to an appropriate sequencing ladder as a size marker.

RESULTS

Length changes in the joining segment between D5 and D6 affect self-splicing rates. These studies of the role of J(56) in the splicing of aI5γ were initiated by constructing length variants of J(56), rather than sequence variants, because the sequence of J(56) in group IIB introns is not highly conserved. A plasmid containing aI5γ plus its flanking exons was mutated so that the wild-type J(56)3 (5′-UUA, positions 849 to 851 of this 887-nt intron) was changed to 0, 1, or 5 nt [J(56)0, J(56)1, and J(56)5, respectively] (Fig. 1). The sequence 5′-UUAUA was chosen for the J(56)5 variant; this allele avoids extending the helix of D6, which might occur if the nucleotides added adjacent to D6 were able to pair with the joining segment connecting D6 with E2. While that situation is potentially interesting per se, its influence would complicate the interpretation of the present study. The J(56)1 mutant retained a single A residue as its J(56); while A might pair with the U preceding D5, that nucleotide was chosen because each of the other possible J(56)1 alleles also might add a base pair to D5 or D6.

These three variant precursor RNAs were found to be detectably reactive in all self-splicing buffers tested, except for the lowest salt condition with 10 mM $MgCl_2$ plus 2 mM spermidine (30). Timed sets of reactions were done in a splicing buffer with 1.5 M $(NH_4)_2SO_4$, and the first-order rate constants are summarized in Table 1. Representative results for the reactions are shown in Fig. 2A. Lanes 1 and 11 illustrate that the wild-type precursor yields spliced exons and intron lariats as the main products; with this high concentration of $(NH_4)_2SO_4$, the spliced exon reopening (SER) reaction converts some of the spliced exon product to separate exon products (21, 29).

These time-series experiments showed that the apparent rate constant for the J(56)0 variant is about 4% of that for the wild-type RNA in $(NH_4)_2SO_4$ splicing buffer (Table 1). Importantly, the array of products obtained with the J(56)0 mutant is strikingly altered (Fig. 2A, lanes 2 to 4), with the clearest differences from the wild-type transcript being the absence of intron lariat and E2 RNAs. This mutation also abolishes branching, but it retains some 5′SJ hydrolysis activity. The mutant RNA also appears to be defective in using the 3′SJ. While the separate 5′ exon product (E1) RNA is present and has the usual length, there is very little RNA migrating near the position of the 3′ exon product (E2) RNA. Linear intermediate (IVS-E2) RNA is also evident in lighter exposures, but the amount of IVS-E2 is not sufficient to account for all of the E1 RNA; therefore, this mutant RNA is not blocked for the second splicing reaction but apparently uses ectopic sites instead. There are some products somewhat larger than E2 that could result from inaccurate 3′SJ selection (see E2* in Fig. 2 and below).

Under the $(NH_4)_2SO_4$ splicing condition, the rate constant of the precursor RNA with the J(56)1 change is about 4% that of the wild-type transcript (Table 1). Like the J(56)0 mutant, the J(56)1 variant forms no lariat RNA, but otherwise its products (Fig. 2A, lanes 5 to 7) closely resemble those of the wild-type precursor (lane 11). However, most splicing occurs at incorrect sites 5′ to the standard 3′SJ (see below).

The J(56)5 variant gave a substantially different result in the $(NH_4)_2SO_4$ splicing buffer. While its splicing rate is about 8% of that of the wild-type RNA, which is only slightly faster than the other two mutants (Table 1), the J(56)5 product array was almost normal, including spliced exon RNAs of apparently correct size and some intron lariat RNA (Fig. 2A, lanes 8 to 10). The J(56)5 lariat RNA was purified and digested by RNase T_1 to release a characteristic branched 12-mer oligonucleotide, just like the wild-type lariat (3, 19). This result indicates that branching occurs at the usual site in D6. The distribution of spliced and separate exons is skewed toward separate exons (relative to the wild-type transcript in lane 11), but splice junction utilization by J(56)5 appears to be accurate (see below).

These three J(56) variant transcripts were also analyzed in 1.5 M KCl splicing buffer. For the wild-type RNA, the KCl reaction buffer permits rapid splicing (see Table 1) but inefficient transesterification in the first step of splicing; in addition, KCl stimulates the SER reaction, so that separate exon products accumulate instead of spliced exons. In the KCl buffer, all three derivatives were nearly as reactive as the wild-type transcript (Table 1). Moreover, while some lariat RNA appears in the reaction with wild-type RNA, only the J(56)5 mutant allele is capable of forming any lariat RNA (Fig. 2B). All three variants show a substantial amount of the linear IVS-E2 reaction intermediate, indicating that the second splicing step is impaired by all three of these mutations. Defects in 3′SJ selection, inferred from the results in Fig. 2A, are now quite apparent for all three mutants in KCl reaction mixtures, on the basis of the accumulation of abnormal products migrating in the vicinity of the normal E2 RNA.

Activation of abnormal 3′ splice sites. Because the accumulation of multiple E2-related products was inferred from the mutant patterns of self-splicing products, several experiments were done to confirm the use of abnormal 3′ splice sites. First, an E2-specific oligonucleotide was used for primer extension by RT of the RNA from 1.5 M KCl splicing reactions (Fig. 3). At least six different lengths for E2 were discernible in the spliced J(56)0 RNA (compare lanes 11 and 12), and this finding agrees generally with the presence of five distinct E2* products in lanes 2 and 3 of Fig. 2B. Accurate splicing accounts for only a small fraction of these 5′ ends (compare lane 6 with lane 12); one site is displaced from the natural 3′SJ by just 2 nt, but several other sites are evident at various locations in D6 (including some that appear to be more frequently used [summarized in Fig. 1]). From the spliced J(56)1 products, some E2 has the canonical 3′SJ as defined by the spliced products from wild-type transcripts (compare lanes 6 and 10), but most of the 5′ ends were displaced into the intron sequence by 1 to 3 nt, and some minor products are even longer (compare lanes 9 and 10). For the spliced J(56)5 RNA (lanes 7 and 8), most of

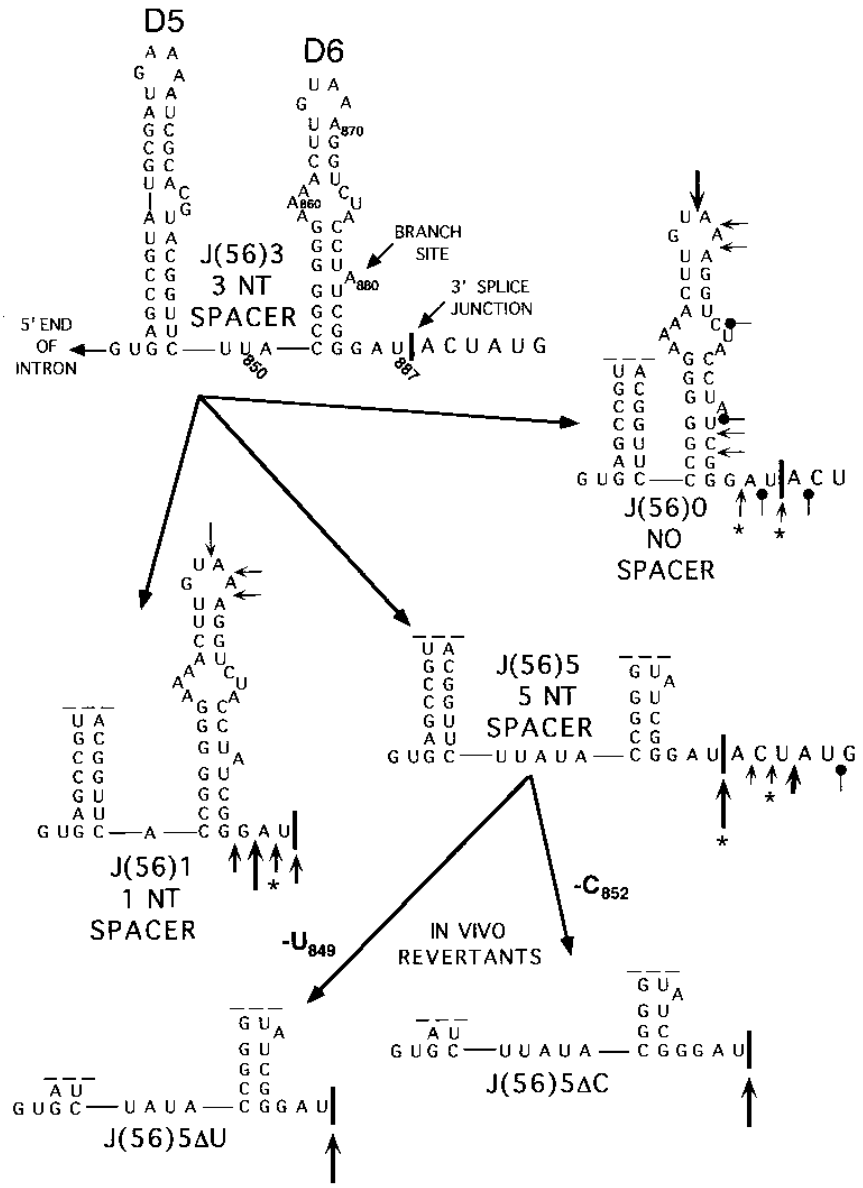

FIG. 1. Sequence and secondary structure of the 3′ segment of wild-type and mutant alleles of aI5γ. The primary sequence and proposed secondary structure of the portion of the wild-type aI5γ including D5, J(56), D6, J(6E2), and part of the downstream exon (E2) are shown at the top. The branch site in D6 (*A*-880) and the location of the 3′SJ are indicated. The middle of the figure shows diagrams defining the J(56)0, J(56)1, and J(56)5 alleles of the intron. Arrows in each diagram of an allele indicate the locations of 3′ splice sites detected by the in vitro reactions for which the results are shown in Fig. 3. The length and thickness of each arrow reflect the relative use of each alternative splice site, and an asterisk indicates that the site was also present in cloned cDNAs from similar in vitro reactions. The cDNAs sequenced included a few other splice sites that were not evident in the experiment of Fig. 3; those sites are indicated by a thin line ending in a filled circle. The J(56)5 mutant allele was transformed into mtDNA in which it showed a substantial splicing defect. The sequences of two types of spontaneous revertants of the J(56)5 mutant are shown at the bottom.

the primer extension signal coincides with the canonical site, but some splicing by J(56)5 is evident at abnormal sites nearby in the E2 sequence (Fig. 1).

The 5′ ends detected by primer extension certainly reflect E2-related products of the self-splicing reactions. We considered it unlikely that the abnormal E2-like RNAs resulted from inaccurate SER activity, because Fig. 2 shows clearly that the E1 RNA produced by these mutant transcripts has the correct length. In order to confirm that these novel E2-related 5′ ends actually resulted from splicing events, cDNAs were amplified by RT-PCR from splicing reactions with E1- and E2-specific primers. When these initial PCR products were analyzed on agarose gels, the majority of the spliced exon cDNA products from the J(56)1 and J(56)5 RNAs were very close to the same length as the cDNA from the J(56)3 transcript (data not shown). By contrast, there was little cDNA of the standard length from the J(56)0 reaction, but a number of longer PCR products were obtained instead. The appearance of all of these cDNAs depended on prior incubation in splicing buffer, RT, and the addition of both primers to the PCR mixtures.

For each transcript, a cDNA fraction was excised from the gel and sequenced with a primer that anneals to the antisense strand of E1. Every cDNA fraction revealed the complete wild-type E1 sequence (data not shown). This result confirms

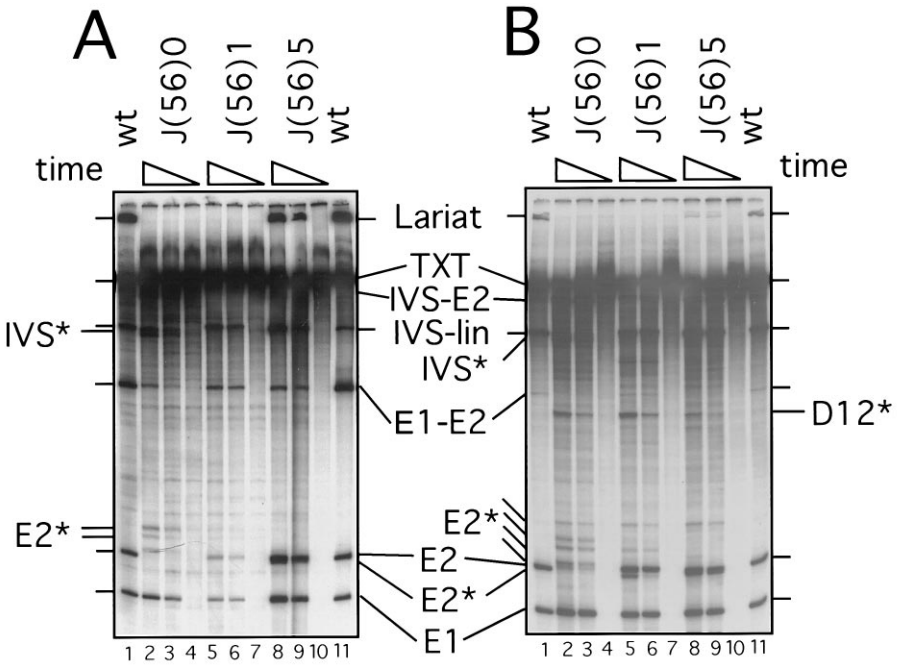

FIG. 2. Self-splicing of pre-mRNAs containing length variants of J(56). (A) Products of self-splicing reactions in buffer containing 1.5 M $(NH_4)_2SO_4$. Labeled pre-mRNAs were reacted in buffer containing 100 mM $MgSO_4$ and 1.5 M $(NH_4)_2SO_4$ at 45°C. Samples were fractionated on a 4% polyacrylamide gel and detected by autoradiography. Lanes 1 and 11 contain wild-type (wt) pre-mRNA [J(56)3] reacted for 5 min. Under this reaction condition, the wild-type RNA yields mostly excised intron lariat and spliced exon RNAs as products; a portion of the spliced exon product is converted to separate E1 and E2 RNAs by the spliced exon reopening reaction. Lanes 2 to 4, 5 to 7, and 8 to 10 illustrate the main products of reactions of J(56)0, J(56)1, and J(56)5 pre-mRNAs, respectively. For each construct, samples were incubated for 0, 15, or 30 min, respectively. Expected product RNAs are labeled between the two panels; these are (from the top) intron lariat (LAR), pre-mRNA (TXT), linear intron-second exon reaction intermediate (IVS-E2), linear intron (IVS-lin), spliced exons (E1-E2), separate second exon (E2), and separate first exon (E1). Novel products include shortened linear intron (IVS*) and second exon RNAs that are shorter or longer than those in the wild-type reactions (E2*). (B) Products of self-splicing reactions in reaction buffer containing 1.5 M KCl. Labeled pre-mRNAs were reacted in buffer containing 100 mM $MgSO_4$ and 1.5 M KCl at 45°C. The reactions were analyzed and displayed as described for panel A. A novel product (D12*) of about 567 nt is evident in the reactions of the mutant RNAs; it results from a postsplicing cleavage at a site in domain 2, as discussed previously (12).

the indication from Fig. 2 that the 5′SJ choice is unaltered by these J(56) length mutations. With the wild-type cDNA, a clear sequence extended beyond E1 into E2. The J(56)5 cDNA sequence was similar to that of the wild type, supporting the conclusion that most of its splicing was accurate. However, the J(56)0 cDNA sequence became heterogeneous immediately after the last nucleotide of E1, indicating that E1 had been spliced to E2-containing segments at many sites. With the J(56)1 cDNA, the sequencing pattern indicated almost no correct splicing, but instead splicing usually occurred with the insertion of 1 or 2 nt derived from the 3′ end of the intron between E1 and E2. These observations demonstrate an allele-specific defect in the accuracy of 3′SJ selection that results from the alterations in the length of J(56).

Next, several cDNAs derived from each of the mutant transcripts were cloned and sequenced. While we did not sequence enough isolates to detect every ectopic E2 site noted in the experiment for which the results are shown in Fig. 3, we confirmed bona fide splicing events for at least one noncanonical 5′ end of E2-related RNAs from each mutant allele (Fig. 1). In addition, several other splice sites that were not prominent in Fig. 3 were also found among the sequenced cDNAs (Fig. 1).

Thermal denaturation properties of D56 RNAs. The substantial activity of all three variants of J(56) in KCl-containing buffers shows that D5 remains functional, so we infer that the D5 secondary structure of each RNA is not significantly altered by any of these J(56) mutations. Since J(56)0 and J(56)1 effectively eliminated the D6 function in step 1, and since both of these alleles have more dramatic effects on branching and on the accuracy of 3′SJ utilization, it seemed possible that these mutations might alter the structure of D6 in some way. To test this possibility, we analyzed the thermal denaturation profiles of RNAs containing D5 and D6 from each J(56) allele. Thermal denaturation was monitored at both 260 and 280 nm, and the resulting transition temperatures (T_m values) are summarized in Table 2.

The wild-type D56 RNA yields a distinctive biphasic melting pattern where the lower and higher T_m values (62.0 and 80.5°C) closely correspond to those of D6 (63.0°C) and D5 (81.0°C), respectively. These findings indicate that the two helical structures do not interact in the wild-type D56 under this condition in any way that alters the T_m of either substructure significantly. These T_m values were wavelength independent, whereas the magnitude of the temperature-induced hyperchromicity at 280 nm exceeded that at 260 nm, as expected for nucleic acids containing G · C base pairs (11).

The melting profiles of D56 RNAs with the J(56)1 or J(56)5 alleles yield transition temperatures resembling those of J(56)3 D56. In the context of this experiment, it is clear that neither of those two joiner mutations significantly alters the stability of D6 or D5. However, the T_m profile of J(56)0 D56 is substantially different from that of wild-type D56, with transitions at 55 and 90°C (Table 1). These changes suggest that J(56)0 D56 has a more stable D5 and a less stable D6 than the wild-type D56. Inspection of the sequence of this D56 allele (Fig. 1) indicates that it could fold to make D5 longer by 2 bp and D6 shorter by 2 bp. In full-length transcripts prepared from the J(56)0 plasmid, such as were used in the experiments for which the results

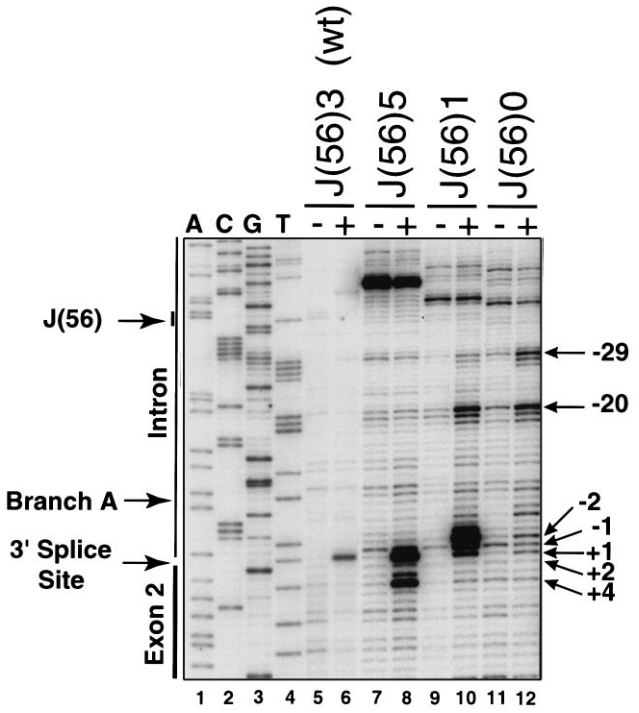

FIG. 3. Survey of 3′ splice sites used by mutant RNAs. RT-primer extension analysis was performed either with unreacted pre-mRNAs (lanes 5, 7, 9, and 11) or with splicing products from 30-min reactions in 1.5 M KCl-containing buffer (lanes 6, 8, 10, and 12) with an oligonucleotide specific for E2. Experiments using wild-type (wt), J(56)5, J(56)1, and J(56)0 RNAs are shown in lanes 5 and 6, 7 and 8, 9 and 10, and 11 and 12, respectively. Lanes 1 to 4 contain the dideoxyribonucleotide sequencing reaction mixtures obtained with pJD20 DNA template by using the same primer. The locations are shown for the standard 3′SJ, the branchpoint in domain 6, and the wild-type J(56) region. The locations of alternative 3′ splice sites used in the various mutants are shown on the right and numbered relative to the wild-type splice site as nucleotide +1; positions within the intron are denoted as negative numbers for which the last intron nucleotide is −1.

are shown in Fig. 2 and Table 1, that folding isomer would not be favored because the 2 nt preceding D5 are GU; in designing the D56 templates, we had changed GU to GG to support better transcription by T7 RNA polymerase (25).

To test the integrity of these D56 RNAs, they were analyzed by *trans* splicing with E1:D123 RNA as the substrate (8, 18). While all of the D56 RNAs were found to be active for E1 release, J(56)0 and J(56)1 totally failed to branch in NH_4Cl reactions, but the wild-type and the three mutants with longer J(56)s (see below) branched to various extents (data not shown). Interestingly, the J(56)0 allele, deduced to have a D5 elongated by 2 bp, clearly retains a functional D5 because it bound well to the substrate and promoted the 5′SJ hydrolysis reaction about as well as wild-type D56 and D5 RNAs. Similarly, an extended D5 RNA specifically designed with an extra 2 bp, ggD5cc, also functions well in this *trans* assay (data not shown).

Effects of J(56)5 mutation on splicing in vivo. The previous sections show that the length of the spacer separating D5 from D6 influences the rate of self-splicing, the extent of branching in the first splicing reaction, and the efficiency and accuracy of the second splicing reaction. Next, we wanted to determine whether the length of the spacer is important for splicing in vivo. In several previous studies, we have found a generally good correlation between in vitro and in vivo phenotypes of mutants in several regions of this intron. The J(56)5 mutant was chosen because it substantially alters the rate of splicing in $(NH_4)_2SO_4$ reactions, while its pattern of products is relatively normal. On the basis of the results obtained with other mutants having similarly reduced rates of self-splicing (4, 28), the J(56)5 variant was anticipated to be splicing defective in vivo.

The J(56)5 allele was transformed into a [*rho*^{0}] yeast strain (a respiration-deficient mutant lacking mtDNA). Test crosses with the resulting synthetic petite mutant showed that the mutant allele does not support splicing. The J(56)5 allele was then transferred by recombination into an otherwise wild-type mtDNA, yielding a *mit*$^-$ mutant strain. RNA blots showed that the mutant has no detectable *COXI* mRNA (Fig. 4A, lane 2) or excised intron RNA (Fig. 4B, lane 2). Most of the hybridization signal in both blots represents the 2.8-kb pre-mRNA containing all of the exons of the *COXI* gene plus aI5γ; however, there is some reaction at the 5′SJ, since a signal appears at the position of the IVS-E2 RNA, as previously characterized from in vivo RNA (28). An RT-PCR experiment was done to produce cDNA copies of in vivo mRNA from the J(56)5 mutant. Although the PCR product was much less abundant than that from wild-type cells, 12 clones of amplified material were recovered and sequenced, and all of them had the wild-type sequence. Thus, the J(56)5 mutation reduces splicing at least 100-fold, to less than the level of detection on Northern blots, but it does not completely abolish accurate splicing.

Sixteen spontaneous revertants of the J(56)5 mutant were isolated, and all were found to grow well on glycerol medium with no detectable conditional phenotype. The D56 region of the intron was sequenced from each revertant strain, and two classes of pseudorevertants were noted, each resulting from a deletion of 1 nt (Fig. 1). Four strains have a 4-nt J(56) with the sequence UAUA, because of the deletion of one of the first two U residues (U_{849} or U_{850}) to yield an allele called J(56)5ΔU. While other secondary structures might be proposed, thermal denaturation of the D56 RNA containing J(56)5ΔU showed that D5 and D6 are as stable in that allele as in the wild type (Table 2). In twelve other strains, 1 of the first 2 nt of D6 (C_{852} or C_{853}) was deleted. Because D6 in the J(56)5ΔC allele is somewhat less stable than that in the wild type (Table 2), it is likely that this mutant retains the 5-nt J(56) but has its D6 shortened by 1 bp. It is curious that this change

TABLE 2. T_m behavior of D5, D6, and D56 RNAs from joiner variant transcripts

Expt no.	J(56) allele	RNA analyzed[a]	Transition temp (°C)[b]	
			Lower	Higher
1		ggD5		81.0
1		ggD5cc		88.0 (+7.0)
1		gguuaD6gau	63.0	
1	J(56)0	ggD5-D6gau	55.0 (−8.0)	90.0 (+9.0)
1	J(56)1	ggD5aD6gau	64.0 (+1.0)	81.0 (0.0)
2	J(56)2	ggD5uaD6gau	61.5 (−1.5)	80.8 (−0.2)
1	J(56)3	ggD5uuaD6gau	62.0 (−1.0)	80.5 (−0.5)
2	(WT)[c]		62.6 (−0.4)	81.1 (+0.1)
2	J(56)5ΔU	ggD5uauaD6gau	64.5 (+1.5)	80.8 (−0.2)
2	J(56)5ΔC	ggD5uuaua$^{\delta C}$D6gau[d]	58.1 (−4.9)	80.8 (−0.2)
2	J(56)5	ggD5uauaD6gau	64.9 (+1.9)	82.3 (+1.3)

[a] Lowercase letters indicate the primary sequences adjacent to D5 and D6.
[b] Numbers in parentheses are ΔT_m values relative to that for gguuaD6gau for the lower temperature transition and relative to that for ggD5 for the higher temperature transition. The data shown are from two separate experiments. The results for J(56)3 (wild type) illustrate the reproducibility of these measurements (31). Underlining indicates controls.
[c] WT, wild type.
[d] ggD5uuaua$^{\delta C}$D6gau is an allele of D56 lacking C_{852}, the first cytosine of D6.

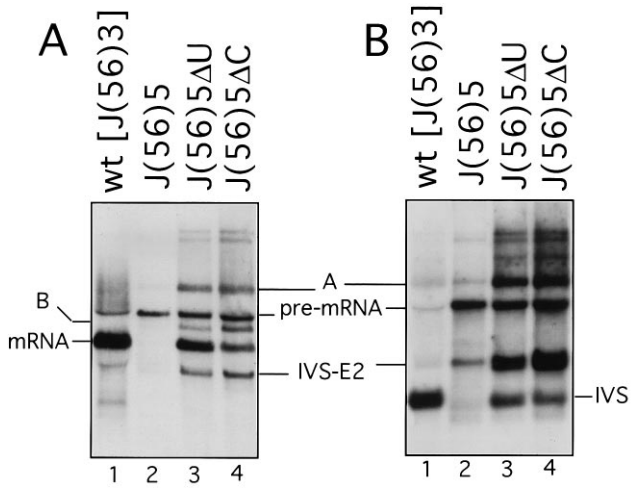

FIG. 4. RNA analysis of splicing in vivo by aI5γ of the *COXI* gene. Total cellular RNA was isolated from cultures of yeast strains grown in raffinose-containing medium carrying the wild-type (wt), J(56)5, J(56)5ΔC, and J(56)5ΔU alleles of intron aI5γ. Samples were fractionated on agarose gels containing formaldehyde, transferred, and hybridized with radiolabeled probes specific for the *COXI* exons (A) or intron aI5γ (B). The same amount of RNA from each preparation was also hybridized with a probe specific for the *COXII* gene, a mitochondrial gene that is transcribed separately from the *COXI* gene. That filter was quantitated, and the relative levels of *COXII* mRNA are 1.0, 0.6, 0.5, and 0.6 for lanes 1 to 4, respectively. The main RNA species are labeled; these are the 2.8-kb pre-mRNA containing *COXI* exons plus aI5γ, the 1.9-kb *COXI* spliced mRNA, and the 0.9-kb excised intron RNA (IVS). IVS-E2 is the partially spliced reaction intermediate; it is most evident in the samples from the mutant strains. Two other RNAs labeled A and B are discussed in the text.

in D6 length partially compensates for the inhibitory effect of lengthening J(56).

Next, the *COXI* transcripts accumulated in the representative pseudorevertant strains were characterized. The RNA blots in Fig. 4 show that the revertants have readily detectable levels of *COXI* mRNA (Fig. 4A, lanes 3 and 4). It is especially evident from Fig. 4B that splicing is still inhibited, because much more unspliced precursor RNA is present in the revertants than in the wild-type strain. Also, about 30% of the unspliced RNA present in each sample is at the position of the IVS-E2 intermediate, indicating that each revertant is rather deficient for the second step of splicing. Two other RNAs are evident in the revertant strains (bands A and B). Band A is probably a pre-mRNA that contains an unspliced intron in addition to aI5γ; in a previous in vivo study of other aI5γ mutant alleles, we noted that the splicing of some other introns can be somewhat slowed (3). Band B is a minor RNA in the pattern of Fig. 4A; since it does not contain aI5γ sequences (compare panels A and B), band B was not characterized further.

Because the J(56)5ΔU and J(56)5ΔC revertants grow well on glycerol medium, at least some of the mRNA must result from accurate splicing. But since three J(56) mutants were shown to have impaired 3′SJ selection in vitro (described above), we tested these partially functional revertants for accurate splicing. RT-PCR was done in four separate trials to amplify cDNAs from spliced mRNAs present in samples of in vivo RNA from the wild-type, J(56)5ΔU, and J(56)5ΔC strains. The resulting material was cloned, and at least three clones were sequenced from each sample of amplified material. Over 20 clones from each revertant were sequenced. All of the clones from the revertants contained the wild-type spliced exon sequence, showing that most, if not all, splicing occurs accurately in these strains.

Both the J(56)5ΔU and J(56)5ΔC alleles were constructed by site-directed mutagenesis from the wild-type plasmid, and in vitro transcripts were analyzed for their patterns and rates of splicing in vitro. As shown in Table 1, both alleles are improved for self-splicing in the $(NH_4)_2SO_4$ buffer by about sixfold compared with their J(56)5 parent, but they remain about twofold slower than the original wild-type transcript. These mutant alleles are quite proficient at executing the first reaction by branching in the $(NH_4)_2SO_4$ buffer, and they even produce some intron lariat in the KCl reaction buffer (data not shown). However, both alleles accumulate measurable amounts of the IVS-E2 intermediate under both reaction conditions, a product that is diagnostic of a decrease in the rate of the second step of splicing. The remaining J(56) length of 2 nt (sequence UA) was also constructed and tested for its rate and pattern of self-splicing (Table 1). The J(56)2-UA allele closely resembled the J(56)5 mutant already analyzed in terms of its pattern of products and rate effects. The product patterns generated by the revertant alleles and the J(56)2-UA variant showed no abnormal RNAs that would suggest a defect in accurate 3′SJ utilization, although the rate decrease noted above suggests some problem in positioning the 3′SJ for step 2 of splicing.

DISCUSSION

The results of this study show that the length of the joiner between D5 and D6 is an important parameter that affects the splicing reactions of a group II intron. Mutations that shorten or lengthen J(56) have dramatic effects on the self-splicing rate under conditions in which the first splicing reaction for the wild-type intron occurs almost exclusively by transesterification [100 mM $MgSO_4$ plus 1.5 M $(NH_4)_2SO_4$]. Two mutants with shortened joiners, J(56)0 and J(56)1, achieve no detectable branching in self-splicing reactions; the J(56)2 mutant makes some lariat product but mostly performs the first reaction by hydrolysis. Those mutant RNAs are blocked for first-step transesterification in KCl-containing reaction mixtures, in which the wild-type transcript yields about 30% intron lariat. Lengthening J(56) to 5 nt reduces the level of branching under both reaction conditions but does not eliminate it. The phenotypes of these mutants are similar to that of the ΔD6 mutant of this intron, from which D6 has been deleted (21). Interestingly, the ΔD6 mutant has a less-deranged phenotype than all but two of the joiner mutations, the two revertants of J(56)5. The results of this study indicate that these J(56) length changes have altered the arrangement of D5 relative to that of D6. Furthermore, this rearrangement has also disturbed the proper relationships of 3′SJ and E2 with the active center of the ribozyme.

From the results of the time course experiments with both reaction buffers, we conclude that all of these joiner mutations substantially inhibit the rate of the second step of splicing. This result is shown by the accumulation of more of the IVS-E2 splicing intermediate than excised intron RNA at short times of reaction. This effect is particularly clear for reactions in KCl-containing buffers, in which the measured rate constant of the first splicing reaction is close to normal. As noted previously for the wild-type intron (16, 17), the first-step reaction is much slower than the second-step reaction. Thus, a rather large decrease in the rate of the second step is required for a given mutation to exert only a small effect on the rate of the first reaction yet lead to accumulation of the IVS-E2 intermediate.

Several of the joiner mutations reduce the accuracy of 3′SJ selection. The J(56)0 mutant is almost completely deficient in using the canonical site. In this mutant, it appears that the

correct arrangement of D5 relative to that of D6, which is evidently needed for accurate splicing, is achieved only rarely. Furthermore, the J(56)0 RNA does not use some alternate splice site consistently; instead, it splices detectably at multiple sites in the vicinity of the canonical 3′SJ (Fig. 1). While the J(56)1 mutant achieves some accurate splicing, most of its splicing occurs at one of several alternate sites within the 3′ sequence of the intron. This may mean that the J(56)1 allele permits a relatively stable arrangement of D5 and D6 that consistently presents the wrong sequence to the second-step active center. In comparison, the ΔD6 mutant is less impaired for 3′SJ selection, with the wild-type splice site being used most of the time (21). The ΔD6 mutant inefficiently uses three alternate sites, two upstream and one downstream of the usual 3′SJ, and one of these alternate sites is the same as the main splice site chosen by the J(56)1 mutant.

The J(56)5 mutant usually splices accurately in vitro, and its rather inefficient splicing in vivo is nevertheless quite accurate. However, some inaccurate splicing occurs in vitro at sites in E2 several nucleotides from the wild-type splice site. Although inaccurate splicing by both the J(56)1 and J(56)5 mutants is within several nucleotides of the wild-type site, the J(56)1 mutant uses sites upstream of the standard site while the J(56)5 mutant uses downstream positions. Presumably, these two J(56) variants convert the 3′ end of the intron to different structures, each competent for accurate first-step reactions but aberrant in distinct ways in the second-step reaction.

If one compares all of the 3′ splice sites used by these three J(56) mutants, ectopic splicing occurs within 13 different trinucleotides (Fig. 1). Because the sequence of the natural 3′SJ (AU|A) is not present except at the usual 3′ end of the intron, all of the alternative splices sites differ by at least one position from this trinucleotide. Earlier research has indicated that the γ-γ′ and internal guide (δ-δ′) interactions are important for 3′SJ selection (15, 17). The wild-type 3′SJ and the upstream nucleotides involved in those interactions are present and unaltered in these J(56) length mutants, but even so the usual 3′SJ is almost completely ignored, especially in J(56)0 and J(56)1 RNAs. Only a few of the alternate sites support both the γ-γ′ or δ-δ′ interactions, but it may be significant that two of those sites [GU|A in J(56)0 and CU|A in J(56)5] are used relatively efficiently. The site used most frequently in J(56)1, GG|A, can support the δ-δ′ interaction. It has also been shown that the first (G_1) and penultimate (*A*-886) intron bases may interact to influence the rate of the second step when splicing proceeds via branched intermediates (6). For the mutants analyzed here, the most efficiently used alternate 3′ splice sites provide relatively poor partners for G_1. However, it is not unexpected that most of the ectopic 3′ splice sites for J(56)0 and J(56)1 do not support the G_1-*A*-886 interaction, since those mutants do not branch at all.

Because J(56)5 usually splices to the wild-type site, it is likely that D5 and D6 interact correctly at least some of the time. The findings that detectable branching occurs in $(NH_4)_2SO_4$ buffer and in *trans* assays (data not shown) also support this idea. Perhaps an additional slow isomerization step for positioning D6 is required for the J(56)5 RNA to undergo transesterification in the first step of splicing. Presumably, the first-step reaction center contains at least E1, D5, and D6. Moreover, the structure of D56 from J(56)5 interferes with binding in *trans*, as shown by a K_m that is severalfold higher than that for wild-type D56 (data not shown). We think it is also likely that the J(56)5 mutation interferes with the formation of the active center for the second step of splicing, presumably containing E1, D5, and the 3′SJ. This reaction center may form slowly, or perhaps E1 and D5 may bind correctly while the site for the 3′SJ remains vacant most of the time. The resulting step 2 delay allows splicing intermediates to accumulate detectably and also permits incorrect RNA sequences to enter the active site and participate in splicing inappropriately.

The in vivo experiments show that a longer joiner is incompatible with efficient splicing. The J(56)5ΔU revertant of J(56)5 probably has a 4-nt joiner. While that mutant allele splices accurately and efficiently enough to support respiratory growth, the RNA blot analysis shows that it remains somewhat defective for splicing, splicing aI5γ from only about 50% of the *COXI* transcripts. Also, the IVS-E2 RNA intermediate is evident, indicating a second-step defect. Similar defects were also noted in the self-splicing reactions of this allele (data not shown). Thus, loss of 1 nt from J(56)5 restores a reasonably efficient reaction in the first step, but that 4-nt joiner still interferes with the second splicing reaction. On the basis of the T_m analysis of its D56 RNA, the other revertant allele, J(56)5ΔC, probably has a modified D6 rather than a shortened J(56) tether (Table 2). The J(56)5ΔC mutant grows well on glycerol medium, and its splicing phenotype is clearly intermediate between those of J(56)5 (splicing negative) and J(56)5ΔU (splicing positive but with a second-step defect). Since the J(56)2 allele is also defective in vitro for splicing in $(NH_4)_2SO_4$ buffer, we conclude that a J(56) of 3 nt provides the optimal separation between D5 and D6 in this intron.

It is interesting that the J(56)2 and J(56)5 mutants splice mostly accurately and with branching in $(NH_4)_2SO_4$ buffer but with substantially reduced rates. This finding suggests that these mutations allow a nearly normal interaction between D5 and D6 but that branchpoint A of D6 is out of position, perhaps only slightly. It would appear that molecules in which D6 is not positioned correctly are prevented from engaging in the first-step reaction by hydrolysis and that they need to move D6 into a more nearly correct position for splicing to be initiated by branching. Notably, increased hydrolysis does not simply compensate for the rate difference when transesterification is slowed by these mutations.

It was anticipated that the results of this study would help us to distinguish between two models for the arrangement of D5 relative to D6. Those models are designated the stacked versus the parallel arrangement of the helices. It seemed likely that shortening J(56) would tend to promote helix stacking at the expense of interactions in parallel. It was found that the three mutants with shortened J(56) sequences had the most-severe negative effects, as assayed by D6 function in branching. Those observations can be interpreted as indicating that D5 and D6 helices probably do not stack in the wild-type RNA.

On the other hand, if D5 and D6 normally align side by side, it seemed likely that lengthening J(56) might not interfere with their interaction, especially if it is stabilized chiefly by specific contacts between residues in D5 and D6. Our findings that a 5-nt J(56) is rather deficient in vitro and is almost totally inactive for splicing in vivo suggest that the interaction between D5 and D6 is not chiefly determined by specific contacts between them. At the outset, we had not considered the possibility that J(56) itself may play a direct role in positioning D5 relative to D6. The notion that J(56) interacts directly with one or both of these two domains is being tested by on-going experiments.

ACKNOWLEDGMENTS

This research was supported by research grants GM31480 from NIH and I-1211 from the Robert A. Welch Foundation to P.S.P. and NP-894 from the American Cancer Society to C.L.P. The Department of Biological Sciences of the University of Pittsburgh provided intramural

research support for the DNA Synthesis Facility and for maintaining the analytical instrumentation.

We thank M. Riley and M. Zhang for expert technical assistance.

REFERENCES

1. **Abramovitz, D. L., R. A. Friedman, and A. M. Pyle.** 1996. Catalytic role of 2′-hydroxyl groups within a group II intron active site. Science **271:**1410–1413.
2. **Belcher, S. M.** 1993. In vivo, in vitro, and reverse genetic studies of splicing of group II introns from yeast mtDNA. Ph.D. dissertation. The University of Texas Southwestern Medical Center, Dallas.
3. **Boulanger, S. C.** 1995. In vitro and in vivo studies of self-splicing group II introns of yeast mtDNA. Ph.D. dissertation. University of Texas Southwestern Medical Center, Dallas.
4. **Boulanger, S. C., S. M. Belcher, U. Schmidt, S. D. Dib-Hajj, T. Schmidt, and P. S. Perlman.** 1995. Studies of point mutants define essential nucleotides in the domain 5 substructure of a group II intron. Mol. Cell. Biol. **15:**4479–4488.
5. **Butow, R. A., S. M. Belcher, J. V. Moran, R. M. Henke, and P. S. Perlman.** 1996. Transformation of *S. cerevisiae* mitochondria using the biolistic gun. Methods Enzymol. **264:**265–278.
6. **Chanfreau, G., and A. Jacquier.** 1993. Interaction of intronic boundaries is required for the second splicing step efficiency of a group II intron. EMBO J. **12:**5173–5180.
7. **Chanfreau, G., and A. Jacquier.** 1994. Catalytic site components common to both splicing steps of a group II intron. Science **266:**1383–1387.
8. **Chin, K., and A. M. Pyle.** 1995. Branch-point attack in group II introns is a highly reversible transesterification, providing a potential proofreading mechanism for 5′-splice site selection. RNA **1:**391–406.
9. **Costa, M., and F. Michel.** 1995. Frequent use of the same tertiary motif by self-folding RNAs. EMBO J. **14:**1276–1285.
10. **Dib-Hajj, S. D., S. C. Boulanger, S. K. Hebbar, C. L. Peebles, J. F. Franzen, and P. S. Perlman.** 1993. Domain 5 interacts with domain 6 and influences the second transesterification reaction of group II intron self-splicing. Nucleic Acids Res. **21:**1797–1804.
11. **Felsenfeld, G., and S. Z. Hirschman.** 1965. A neighbor-interaction analysis of the hypochromism and spectra of DNA. J. Mol. Biol. **13:**407–427.
12. **Franzen, J. F., M. Zhang, and C. L. Peebles.** 1993. Kinetic analysis of the 5′ splice junction hydrolysis of a group II intron promoted by domain 5. Nucleic Acids Res. **21:**627–634.
13. **Franzen, J. S., M. Zhang, T. R. Chay, and C. L. Peebles.** 1994. Thermal activation of a group II intron ribozyme reveals multiple conformational states. Biochemistry **33:**11315–11326.
14. **Jacquier, A.** 1990. Self-splicing group-II and nuclear pre-messenger RNA introns—how similar are they? Trends Biochem. Sci. **15:**351–354.
15. **Jacquier, A., and N. Jacquesson-Breuleux.** 1991. Splice site selection and role of the lariat in a group II intron. J. Mol. Biol. **219:**415–428.
16. **Jacquier, A., and F. Michel.** 1987. Multiple exon-binding sites in class II self-splicing introns. Cell **50:**17–29.
17. **Jacquier, A., and F. Michel.** 1990. Base-pairing interactions involving the 5′ and 3′ terminal nucleotides of group II self-splicing introns. J. Mol. Biol. **213:**437–447.
18. **Jarrell, K. A., R. C. Dietrich, and P. S. Perlman.** 1988. Group II intron domain 5 facilitates a *trans*-splicing reaction. Mol. Cell. Biol. **8:**2361–2366.
19. **Jarrell, K. A., C. L. Peebles, R. C. Dietrich, S. L. Romiti, and P. S. Perlman.** 1988. Group II intron self-splicing: alternative reaction conditions yield novel products. J. Biol. Chem. **263:**3432–3439.
20. **Kim, S.-H., F. L. Suddath, G. J. Quigley, A. McPherson, J. L. Sussman, A. Wang, N. Seeman, and A. Rich.** 1974. Three-dimensional tertiary structure of yeast phenylalanine transfer RNA. Science **185:**435–440.
21. **Koch, J. L., S. C. Boulanger, S. D. Dib-Hajj, S. K. Hebbar, and P. S. Perlman.** 1992. Group II introns deleted for multiple substructures retain self-splicing activity. Mol. Cell. Biol. **12:**1950–1958.
22. **Madhani, H. D., and C. Guthrie.** 1992. A novel base-pairing interaction between U2 and U6 snRNAs suggest a mechanism for the catalytic activation of the spliceosome. Cell **71:**803–817.
23. **Michel, F., and J. L. Ferat.** 1995. Structure and activities of group II introns. Annu. Rev. Biochem. **64:**435–461.
24. **Michel, F., K. Umesono, and H. Ozeki.** 1989. Comparative and functional anatomy of group II catalytic introns—a review. Gene **82:**5–30.
25. **Milligan, J. F., and O. C. Uhlenbeck.** 1989. Synthesis of small RNAs using T7 RNA polymerase. Methods Enzymol. **180:**51–62.
26. **Murphy, F. L., Y.-H. Wang, J. D. Griffith, and T. R. Cech.** 1994. Coaxially stacked RNA helices in the catalytic center of the *Tetrahymena* ribozyme. Science **265:**1709–1712.
27. **Padgett, R. A., M. Podar, S. C. Boulanger, and P. S. Perlman.** 1994. The stereochemical course of group II intron self-splicing. Science **266:**1685–1688.
28. **Peebles, C. L., S. M. Belcher, M. Zhang, R. C. Dietrich, and P. S. Perlman.** 1993. Mutation of the conserved first nucleotide of a group II intron from yeast mitochondrial DNA reduces the rate but allows accurate splicing. J. Biol. Chem. **268:**11929–11938.
29. **Peebles, C. L., E. A. Benatan, K. A. Jarrell, and P. S. Perlman.** 1987. Group II intron self-splicing: development of alternative reaction conditions and identification of a predicted intermediate. Cold Spring Harbor Symp. Quant. Biol. **52:**223–232.
30. **Peebles, C. L., P. S. Perlman, K. L. Mecklenburg, M. L. Petrillo, J. H. Tabor, K. A. Jarrell, and H.-L. Chen.** 1986. A self-splicing RNA excises an intron lariat. Cell **44:**213–223.
31. **Peebles, C. L., M. Zhang, P. S. Perlman, and J. F. Franzen.** 1995. Catalytically critical nucleotides in domain 5 of a group II intron. Proc. Natl. Acad. Sci. USA **92:**4422–4426.
32. **Perlman, P. S.** 1990. Genetic analysis of RNA splicing in yeast mitochondria. Methods Enzymol. **181:**539–558.
33. **Pley, H. W., K. M. Flaherty, and D. B. McKay.** 1994. Three-dimensional structure of a hammerhead ribozyme. Nature (London) **372:**68–74.
34. **Podar, M., P. S. Perlman, and R. A. Padgett.** 1995. Stereochemical selectivity of group II intron splicing, reverse splicing, and hydrolysis reactions. Mol. Cell. Biol. **15:**4466–4478.
35. **Poutre, C., and T. D. Fox.** 1987. PET111, a *Saccharomyces cerevisiae* nuclear gene required for the translation of the mitochondrial mRNA encoding cytochrome c oxidase subunit II. Genetics **115:**637–647.
36. **Pyle, A. M., and J. B. Green.** 1994. Building a kinetic framework for group II intron ribozyme activity: quantitation of interdomain binding and reaction rate. Biochemistry **33:**2716–2725.
37. **Schmitt, M. E., T. A. Brown, and B. L. Trumpower.** 1990. A rapid and simple method for preparation of RNA from *Saccharomyces cerevisiae*. Nucleic Acids Res. **18:**3091–3092.
38. **van der Veen, R., A. C. Arnberg, G. van der Horst, L. Bonen, H. F. Tabak, and L. A. Grivell.** 1986. Excised group II introns in yeast mitochondria are lariats and can be formed by self-splicing in vitro. Cell **44:**225–234.